Structural Eng./Earthquake Eng. Vol. 10, No. 1, 23s—33s, April 1993
Japan Society of Civil Engineers (Proc. of JSCE No. 465/I—23)

2-D ELASTODYNAMIC FUNDAMENTAL SOLUTION FOR DISTRIBUTED LOADS AND BEM TRANSIENT RESPONSE ANALYSES OF HALFPLANE PROBLEMS

Hirokazu TAKEMIYA*, Canyun WANG**
and Akihiro FUJIWARA***

A closed form solution for the 2-dimensional problem to evaluate the displacement and stress of an elastic fullspace subject to sudden distributed forces is developed. The force is expressed in a form of multinormal function of space and time variables over strips and time increments. The solution procedure is to utilize the Fourier-Laplace domain transform with the Cagniard-de Hoop method for the inversion. The application to the boundary-initial value problems is demonstrated for the Lamb's problem and for the seismic wave scattering propagation problem. The former makes the validation of the present solution and the latter provides the useful information on ground motions at irregular sites.

Key Words : *2-D elastodynamics, fundamental solution, distributed load, time-domain BEM, Labmb's problem, seismic wave scattering*

1. INTRODUCTION

Currently, various boundary element methods (BEM) are extensively used for the analysis of elastodynamic problems of infinite boundary. In the earthquake engineering field, the irregular site response analysis and the soil structure interaction problems which precludes the analytical solution, are the most successfully applied area among others.

Since the pioneering work by Cruse and Rizzo[1] (1968) which utilized the Laplace transform to solve a halfplane wave propagation due to a surface loading (Lamb's problem[2], 1904), a modified version was developed by Manolis and Beskos[3] (1981), and the Fourier synthesis approach was taken for the steady state harmonic solution by Niwa et al[4] (1976). A direct time domain procedure, on the other hand, was shown by Cole et al[5] (1978) for the analysis of transient antiplane motions with explicit time stepping scheme. The similar technique is used by Niwa et al[6] (1980) who employed the simpler three dimensional fundamental solution for the two-dimensional plane stree/plane strain cases. Manolis[7] (1983) performed a comparative study on the frequency and time domain BEMs for the wave scattering and propagation around a cylindrical cavity in the medium under a specified wave incidence. Karabalis and Beskos[8] (1984) computed an impulse response of a surface rigid body. Mansur and Brebbia[9] (1985) formulated the time domain boundary element method in the same scheme for a scalar wave problem.

Compared to the frequency domain approach, the direct time domain method is more suited to the boundary-initial value problems in elastodynamics. The fundamental solution for a point load to a full space constitutes displacement and traction kernels in the boundary integral equation. The time domain BEM formulation, after discretization by introducing polynomial interpolation functions, involves the elementwise double convolution integral both in time and space variables on such kernels. The conventional procedures have taken the numerical quadrature for the space integration and the analytical time stepping algorithm for the time convolution integral. Besides the singularity in the fundamental solution, special care should be taken in the integration process for the causality condition. Israil and Banerjee[10] (1982) derived an explicit form for this. Mansur[11] (1985) took a complicated manipulation of the Heaviside function for the traction kernel, which is still implicit since it is based on the prior assumption on temporal displacement variation. Wang and Takemiya[12] (1992) have developed an analytical solution method for the 2-dimensional scalar wave problem through the integral transform procedure with use of the Cagniard de-Hoop technique[13] (1959/1960). We can note that the above integral is tantamount to evaluating the Green function for a distributed force whose description is given by multinormal functions.

The Navier equation for the in-plane motion of an elastic medium is governed by a coupled shear (S-wave) and pressure wave (P-wave) field. Introducing the displacement potential function separates the wave field is split into the indepen-

* Prof., Dept. of Civ. Engrg., Okayama Univ., Okayama 700, Japan
** Formerly graduate student, Research fellow Northwestern Univ.
*** Graduate student

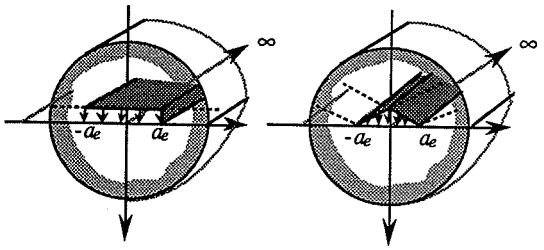

(a) Uniform load (b) Linear load

Fig.1 Strip loading to an elastic fullspace

dent Helmholtz equations concerning these. For the plane wave problem, these result in the scalar wave equations. The characteristic feature of the inplane motion, in contrast to the out-of-plane motion, is that the wave potentials are differentiated for displacement and then for the stress computation. Using the Knopoff-de Hoop representation for the displacement response, the triple convolution integrals appear with respect to time and space. These operations are conducted in the Fourier and Laplace transformed domain, so that the result is inverted back into the space and time. The coordinate transformation is also needed from the local to the global coordinates on these vector quanities. The time-stepping scheme is implemented for the transient response analysis for arbitrary time functions. The substructure method simplifies the response computation for coupled different domains.

For the validation of the present method, an illustrative example of a Lamb problem is first solved, and then the transient wave scattering/ propagation due to the irregular site configuration is investigated for a presumed incident wave.

2. MULTINORMALLY DISTRIBUTED FORCE

Suppose an isotropic, homogeneous, linear infinite elastic solid subjected to a strip force, without losing generality, which spans over a width $2a_e$ on the x-axis, placed on $z=0$ and is distributed identical all along the third axis as illustrated in **Fig.1**. We can give a mathematical expression to it by introducing the Dirac's delta function $\delta(\ )$, the distribution function $f(x, t)$ and the vector intensity $\boldsymbol{a}$ as

$$\boldsymbol{f}(x, z, t)=\boldsymbol{a}f(x, t)\delta(z) \cdots\cdots (1)$$

In the modern numerical method for continuum analysis, we approximate the original continuous displacement and traction distribution in space and time by piecewise continuous simple algebraic expressions. For instance, for the spatial configuration, by introducing the Heaviside step function $H(\ )$ and the *sgn* function such that

$$H(\pm a_e)=H(\xi+a_e)-H(\xi-a_e) \cdots\cdots (2)$$

$$q_{M\pm}=\frac{1}{a_e^m}(\xi\pm a_e)^m sgn(\xi\pm a_e),\ m=0,1,2. \cdots\cdots (3)$$

we define the following interpolation functions : For a constant disribution with width $2a_e$

$$\phi_1^0=H(\pm a_e)=\frac{1}{2}(q_{0+}-q_{0-}) \cdots\cdots (4)$$

for a linear distribution over the $2a_e$

$$\phi_1^1=\frac{1}{2a_e}(a_e-\xi)H(\pm a_e)$$

$$=\frac{1}{4}(q_{1+}-q_{1-})+\frac{1}{2}q_{0+} \cdots\cdots (5\text{-a})$$

$$\phi_2^1=\frac{1}{2a_e}(a_e+\xi)H(\pm a_e)$$

$$=\frac{1}{4}(q_{1+}-q_{1-})-\frac{1}{2}q_{0+} \cdots\cdots (5\text{-b})$$

and etc. as indicated in the authors' previous work (Wand and Takemiya[12], 1992). Quite similarly, the discretization for the time variation is described by changing the width $2a_e$ by the time increment Δt in the respective expression.

The above expressions suggest that the forcing function may be described by a liner combination of multinormal functions over a finite space variable and time segment of $(d_1, d_2, ; t_1, t_2)$ in a generalized form, i.e.,

$$f(x, t)=\sum_{m=0}^{M}\sum_{n=0}^{N} b^{mn}x^m t^n \{H(x-d_1)-H(x-d_2)\}\{H(t-t_1)-H(t-t_2)\} \cdots\cdots (6)$$

This is arranged into a set of functions defined in $(-\infty, +\infty ; 0, +\infty)$ for convenience of the later use.

$$f(x,t)=\sum_{m=0}^{M}\sum_{n=0}^{M}\left\{\sum_{i=1}^{2}\sum_{j=1}^{2} c_{ij}^{mn} f^{mn}(x-d_i, t-t_j)\right\} \cdots\cdots (7)$$

in which

$$c_{ij}^{mn}=\sum_{p=m}^{M}\sum_{q=n}^{N}(-1)^{i+j}b^{p,q}\begin{bmatrix}p\\m\end{bmatrix}\begin{bmatrix}q\\n\end{bmatrix}d_i^{p-m}t_j^{q-n} \cdots\cdots (8)$$

and

$$f^{mn}(x, t)=X^m(x)T^n(t)$$

$$\text{with } X^m(x)=sgn(x)x^m \text{ and } T^n(t)=t^nH(t) \cdots\cdots (9)$$

The terms $\begin{bmatrix}p\\m\end{bmatrix}$ and $\begin{bmatrix}q\\n\end{bmatrix}$ stand for the binomial coefficients ; M and N are the total numbers of superposition of the functions involved.

3. RESPONSE EVALUATION

In order to formulate the two-dimensional wave field due to line source, fist consider the constituent wave potential equation.

$$\left(\nabla^2-\frac{\partial^2}{\partial t_\alpha^2}\right)V(r,t_\alpha)=-\delta(x)\delta(z)\delta(t),$$

$\alpha=1$ or 2 ..... (10)

in which $t_\alpha=c_\alpha t$, $\alpha=1,2$ indicates the P and S wave respectively and c_1 and c_2 denote the associated wave velocities, $r=\sqrt{x^2+z^2}$ is the distance from source to a field point and $\nabla^2=\partial^2/\partial x^2+\partial^2/\partial z^2$ defines the Laplacian operator. The potential function $V(r,t_\alpha)$ is the solution of the Helmholtz equation, Eq.(10), so that

$$V(r,t_\alpha)=\frac{H(t_\alpha-r)}{2\pi(t_\alpha^2-r^2)^{1/2}} \text{ with } t_\alpha=c_\alpha t \cdots\cdots (11)$$

The associated displacement (fundamental solution) takes the expression of

$$\rho U_{\alpha\beta}=\frac{1}{c_1^2}\int_0^{t_1}V_{,\alpha\beta}(r,t_1-\tau_1)\tau_1 d\tau_1$$
$$-\frac{1}{c_2^2}\int_0^{t_2}V_{,\alpha\beta}(r,t_2-\tau_2)\tau_2 d\tau_2+\frac{\delta_{\alpha\beta}}{c_2^2}V(r,t_2)$$
$$=\frac{1}{c_1^2}V_{,\alpha\beta}(r,t_1)*t_1-\frac{1}{c_2^2}V_{,\alpha\beta}(r,t_2)*t_2$$
$$+\frac{\delta_{\alpha\beta}}{c_2^2}V(t,t_2) \cdots\cdots (12)$$

in which the symbol $*$ designates the convolution integral in time t_α; $\alpha,\beta=1,2$ designate the coordinates. These subscripts behind the comma means taking derivative with respect to these variables. Following the Knopoff-De-Hoop representation theorem, the displacements due to the force $f(x,t)\,\boldsymbol{a}_\beta$ are given in the convolution integral form with the aid of the fundamental solution $\boldsymbol{U}_{\alpha\beta}$, as

$$\boldsymbol{u}_{\alpha\beta}(x,z,t)=\int_{-\infty}^{\infty}\int_0^t \boldsymbol{U}_{\alpha\beta}(x-\xi,z,t-\tau) f(\xi,\tau)\,d\tau d\xi$$
$$=\boldsymbol{U}_{\alpha\beta}(x,z,t)*\boldsymbol{f}(x,t) \cdots\cdots (13)$$

The associated stresses are calculated from the knowledge of elasticity.

$$\sigma_{\alpha\beta\gamma}=\rho(c_1^2-2c_2^2)\boldsymbol{u}_{\chi\tau,\chi}\delta_{\alpha\beta}+\rho c_2^2(\boldsymbol{u}_{\alpha\tau,\beta}+\boldsymbol{u}_{\beta\tau,\alpha}) \cdots\cdots (14)$$

where γ indicates the plane of force application, whose direction cosine is given by n_τ. The traction on the surface of normal direction n_τ is found from the stress components by the formula.

$$t_{\alpha\beta}=n_\tau\sigma_{\alpha\beta\tau} \cdots\cdots (15)$$

The convolution expression for response due to the strip loads of Ed.(9) is now formulated, by substituting Eq.(12) for the Green function into Eq.(13) as

$$\rho\boldsymbol{u}_{\alpha\beta}^{m,n}=\left[\frac{1}{c_1^{n+2}}X^m(x)*V(r,t_1)*t_1\cdot T^n(t_1)\right.$$
$$-\frac{1}{c_2^{n+2}}X^m(x)*V(r,t_2)*t_2*T^n(t_2)$$
$$\left.+\frac{\delta_{\alpha\beta}}{c_2^{n+2}}X^m(x)*V(r,t_2)*T^n(t_2)\right]_{,\alpha\beta}$$
$$\cdots\cdots (16)$$

Now we define the following convenient fundamental double convolution integral pair among wave potential and force distribution in space and time ; and also the the derivative with respect to the variable z, i.e.,

$$\boldsymbol{R}^{m,n}=\{P^{mn},Q^{mn}\}=\left\{1,\frac{\partial}{\partial z}\right\}X^m(x)$$
$$*V(x,z,t_\alpha)*T^n(t_\alpha) \cdots\cdots (17)$$

The explicit expressions for displacements and stresses in terms of this definition appear in Appendix A.

In view of the symmetric nature of the problem for **Fig.1**, we state that

$$\boldsymbol{R}^{mn}=\{P^{mn}(x,z,t_\alpha),Q^{mn}(x,z,t_\alpha)\}$$
$$=sgn(x^{m+1})\{P^{mn}(|x|,|z|,|t_\alpha|),$$
$$sng(z)Q^{mn}(|x|,|z|,|t_\alpha|)\} \cdots\cdots (18)$$

The solution procedure for this is to apply the Cagniardde-de Hoop method and was detailed in the authors' publication[12] and is omitted here. The singularity at the wave front is treated completely analytically in the formulation. The results are expressed as follows :

$$P^{mn}=sgn(x^{m+1})[A_0^{mn}H(t_\alpha-|z|)+\frac{1}{\pi}\{A_1^{m,n}f_1$$
$$+A_2^{mn}f_2+A_3^{mn}f_3+A_4^{mn}f\}]H(t_\alpha-r) \cdots\cdots (19)$$
$$Q^{mn}=sgn(x^{m+1})[B_0^{mn}H(t_\alpha-|z|)$$
$$+\frac{1}{\pi}\{B_1^{mn}f_1+B_2^{mn}f_2+B_3^{mn}f_3$$
$$+B_4^{mn}f_4\}]H(t_\alpha-r) \cdots\cdots (20)$$

in which

$$f_1=\tan^{-1}\frac{\sqrt{t_\alpha^2-r^2}}{|x|},\ f_2=\tan^{-1}\frac{|z|\sqrt{t_\alpha^2-r^2}}{|x|\tau},$$
$$f_3=\cosh^{-1}\frac{t_\alpha}{r},\ f_4=\tan^{-1}\sqrt{t_\alpha^2-r^2},$$
and $r^2=x^2+z^2$

The coefficients A and B are multinormal functions of x,z and t. Hence, displacements are obtained from Eq.(13) by viewing Eq.(18) and stresses are obtained after substituting these into Eq.(14). Note that the causality is fully taken into account for the

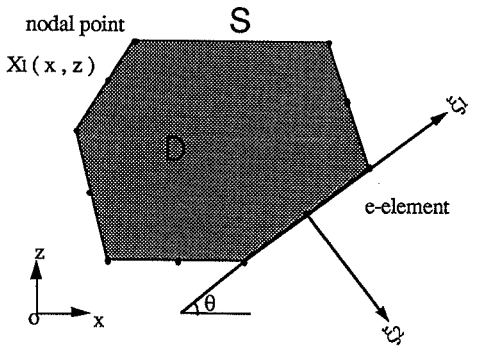

Fig.2 Discretization by straight line elements and global and local coordinate systems.

P and S wave propagation.

4. BOUNDARY ELEMENT EQUATION

The boundary integral equation for elastodynamic problems is described by

$$\varepsilon_{\alpha\beta}(\boldsymbol{x})\boldsymbol{u}_\alpha(\boldsymbol{x},t)=\int_b \boldsymbol{U}_{\alpha\beta}(\boldsymbol{y},t;\boldsymbol{x})*\boldsymbol{t}_\alpha(\boldsymbol{y},t)\,db(\boldsymbol{y})$$
$$-p.v.\int_b \boldsymbol{T}_{\alpha\beta}(\boldsymbol{y},t;\boldsymbol{x})*\boldsymbol{u}_\alpha(\boldsymbol{y},t)\,db(\boldsymbol{y})\cdot(21)$$

in which $\boldsymbol{U}_{\alpha\beta}$ and $\boldsymbol{T}_{\alpha\beta}$ denote, respectively, the displacement fundamental solution (Green function) for an impulsive point force application and the associated traction, and the integral with the notion of $p.v.$ means the integral in the sense of Cauchy's principal value. The term $\varepsilon_{\alpha\beta}(\boldsymbol{x})$, due to the singularity of the traction Green function $\boldsymbol{T}_{\alpha\beta}$, concerns the geometry of the boundary. The discretization of the boundary is performed into E numbers of straight line elements, as illustrated in **Fig.2**, each of which has $M+1(M=0, 1, 2)$ nodal points within it. The total numbers of nodal points is counted by $L=E$ when $M=0$; when $M\geq 1$, $L=M\times E+1$ for a closed boundary and $L=M\times E+1$ for an open boundary problem.

The displacement and traction in the e-th element is approximated by an introduced interpolation function ϕ for space variable and the concerned nodal values. When the isoparametric elements are used, these are expressed as

$$\{\boldsymbol{u}^e(\xi,t),\boldsymbol{t}^e(\xi,t)\}=\sum_{m=1}^{M+1}\phi_m^M(\xi)$$
$$\{\boldsymbol{u}^{e,m}(t),\boldsymbol{t}^{e,m}(t)\}\cdots\cdots(22)$$

in which ξ is the local coordinate attached to the e-th element. The interpolation function is mostly specified by a constant, linear or quadratic variation. Substituting Eq.(22) into Eq.(21) yields

$$\varepsilon(\boldsymbol{x})\boldsymbol{u}_{\alpha\beta}(\boldsymbol{x},t)=\sum_{e=1}^{E}\sum_{m=1}^{M+1}\int_{-a_e}^{a_e}\boldsymbol{U}_{\alpha\beta}(\boldsymbol{y},\boldsymbol{t};\boldsymbol{x})$$
$$\phi_m^M(\xi)J_e(\xi)\,d\xi*\boldsymbol{t}_\alpha^{e,m}(t)$$
$$-\sum_{e=1}^{E}\sum_{m=1}^{M+1}p.v.\int_{-a_e}^{a_e}\boldsymbol{T}_{\alpha\beta}(\boldsymbol{y},\boldsymbol{t};\boldsymbol{x})\phi_m^M(\xi)$$
$$J_e(\xi)\,d\xi*\boldsymbol{u}_\alpha^{e,m}(t)\,d\xi(y)\cdots\cdots(23)$$

in which $J_e(\xi)$ defines the Jacobian that results from the coordinate transformation from local to global system. In a matrix form Eq.(23) becomes

$$\boldsymbol{CU}(t)=\boldsymbol{G}(t)*\boldsymbol{T}(t)-\boldsymbol{H}(t)*\boldsymbol{U}(t)\cdots\cdots(24)$$

with

$$\boldsymbol{U}(t)=\{u_1(\boldsymbol{x}_1)u_2(\boldsymbol{x}_1)\cdots u_1(\boldsymbol{x}_L)u_2(\boldsymbol{x}_L)\}^T\cdots(25)$$

$$\boldsymbol{T}(t)=\{t_1(\boldsymbol{x}_1)t_2(\boldsymbol{x}_1)\cdots t_1(\boldsymbol{x}_L)t_2(\boldsymbol{x}_L)\}^T\cdots\cdots(26)$$

and $\boldsymbol{C}$ being the diagonal matrix of $C_{2l-\alpha,2l-\beta}=C_{\alpha\beta}(\boldsymbol{x}_l)$ for the position vector $\boldsymbol{x}_l$ of the nodal number l due to the singularity of the traction Green function. $\boldsymbol{G}$ and $\boldsymbol{H}$ are $2L\times 2L$ matrices whose description is obvious from Eq.(23). Also, the time discretization is conducted, by introducing the interpolation function $\varphi^u(t)$ and $\varphi^t(t)$ for displacenement and traction respectively, as

$$\{\boldsymbol{U}(t),\boldsymbol{T}(t)\}=\sum_k\{\varphi_k^u(t)\boldsymbol{U}^k,\varphi_k^t(t)\boldsymbol{T}^k\}$$
$$\cdots\cdots(27)$$

therefore, Eq.(24) becomes

$$\boldsymbol{CU}^k=\sum_k\left\{\left[\int_0^{t_k}\boldsymbol{G}(t_k-t)\varphi_k^t(t)\,dt\right]\boldsymbol{T}^k\right.$$
$$\left.-\left[\int_0^{t_k}\boldsymbol{H}(t_k-t)\varphi_k^u(t)\,dt\right]\boldsymbol{U}^k\right\}\cdots\cdots(28)$$

In order to utilize the translation property of the convolution integral and to decouple the preceding solution from the future ones, we can assume that

$$\varphi_k^t(t)=\begin{cases}\varphi(t-t_k) & \text{for } t_k-\Delta t\leq t\leq t_k+\Delta t\\ 0 & \text{otherwise}\end{cases}\quad(29)$$

Only a constant or a linear function whose description is given by

$$\varphi^0(t)=H(t)-H(t-\Delta t)\cdots\cdots(30\text{-a})$$

$$\varphi^1(t)=\frac{1}{\Delta t}\{(t+\Delta t)H(t)-2tH(t)$$
$$+(t-\Delta t)H(t-\Delta t)\}\cdots\cdots(30\text{-b})$$

satisfies the above condition. With this interpolation function, we get a time stepping algorithm for the governing equation.

$$\boldsymbol{H}^0\boldsymbol{U}^k-\boldsymbol{G}^0\boldsymbol{T}^k=-\sum_{k=1}^{K-1}(\boldsymbol{H}^{K-k}*\boldsymbol{U}^k-\boldsymbol{G}^{K-k}*\boldsymbol{T}^k)$$
$$=-\boldsymbol{F}^K\cdots\cdots(31)$$

in which $\boldsymbol{G}^k$ and $\boldsymbol{H}^k$ are defined as

$$\{\boldsymbol{H}^k\boldsymbol{G}^k\}=\left\{\delta_k\boldsymbol{C}+\int_{-\Delta t}^{\Delta t}\boldsymbol{H}(t_k-t)\varphi_k^u(t)\,dt\right.$$
$$\left.\int_{-\Delta t}^{\Delta t}\boldsymbol{G}(t_k-t)\varphi_k^t(t)\,dt\right\}\cdots\cdots(32)$$

with $\delta_k=1$ for $k=0$, and $\delta_k=0$ otherwise. Evaluating the involved matrices $\boldsymbol{G}^k$ and $\boldsymbol{H}^k$ needs the following integral operation.

$$\boldsymbol{V}^{M,N}_{\alpha,\beta}(l,e|m,k)=\int_{-ae}^{ae}\int_{-\Delta t}^{\Delta t}\{\boldsymbol{U}_{\alpha\beta}(y(\xi),t_k-t;x_l);\boldsymbol{T}_{\alpha\beta}(y(\xi),t_k-t;x_l)\}\phi^M_m(\xi)\varphi^N_m(t)J_e(\xi)dtd\xi \quad \cdots\cdots(33)$$

in which "l" specifies the forcing element while "e" the field element. Attention should be paid to that the singularity term once excluded in the above is brought back inside the integral and it is executed analytically by the integral transform procedure. This elementwise and time stepwise integral is closely related to the fundamental convolution integral as described in the succeeding section.

5. FUNDAMENTAL CONVOLUTION INTEGRAL

Under the straight line discretization, the elementwise double integral $\bar{\boldsymbol{V}}^{M,N}_{k\tau}(\xi,t_k|e,m)$ in Eq.(33) is evaluated on the local coordinates $\xi=(\xi_1,\xi_2)$, by

$$\bar{\boldsymbol{V}}^{M,N}_{k\tau}(\xi,t_k|e,m)=\int_{-ae}^{ae}\int_{-\Delta t}^{\Delta t}\{U_{k\tau}(\xi_1-\chi,\xi_2;t_k-s);T_{k\tau}(\xi_1-\chi,\xi_2;t_k-s)\}\phi^M_m(\chi)\bar{\varphi}^N_m(s)d\chi ds \quad \cdots\cdots(34)$$

which is viewed as the response for the forcing function to be given by the product of space and time interpolation functions. We can use the following expression for this by recalling Eq.(7).

$$\phi^M(\chi)\varphi^N(s)=\sum_{m=0}^{M}\sum_{n=0}^{N}\sum_{i=1}^{2}\sum_{j=1}^{1}b^{mn}_{ij}f^{mn}[(\chi-(-1)^i a_e),(s-j\Delta t)] \quad (M=0,1;N=0,1,2) \quad \cdots\cdots(35)$$

in which the coefficient b^{mn}_{ij} is properly determined. The Eq.(34) now needs the computation of

$$\boldsymbol{R}^{m,n}_{k\tau}=\int_{-\infty}^{\infty}\int_{-\Delta t}^{\Delta t}\{U_{k\tau}(\xi_1-\chi,\xi_2;t-s),T_{k\tau}(\xi_1-\chi,\xi_2;t-s)\}f^{mn}(\chi,s)dsd\chi \quad \cdots\cdots(36)$$

which is conducted analytically. Since the wave potential solution in Eq.(11) is related to $\boldsymbol{U}_{k\tau}$ and $\boldsymbol{T}_{k\tau}$ through Eq.(12) and, Eqs.(13) and (14) in the local coordinates, the expression of Eq.(36) is provided with terms of $P^{m,n}$ and $\boldsymbol{Q}^{m,n}$ in Eqs.(19) and (20). Hence, we get from the superposition principle that

$$\bar{\boldsymbol{V}}^{M,N}_{k\tau}=\sum_{m=0}^{M}\sum_{n=0}^{N}\sum_{i=1}^{2}\sum_{j=1}^{1}b^{mn}_{ij}\boldsymbol{R}^{mn}_{k\tau} \quad \cdots\cdots(37)$$

The explicit expressions are given in Appendix B by introducing a new matrix $\boldsymbol{R}^{m,n}_{k\pm}$ matrix such that

$$\boldsymbol{R}^{m,n}_{k\pm}=\frac{1}{a_e\Delta t^N}\begin{bmatrix}R^{m,n}_{11}(\xi_1+a_e,\xi_2,t_k) & R^{m,n}_{12}(\xi_1+a_e,\xi_2,t_k)\\ R^{m,n}_{21}(\xi_1+a_e,\xi_2,t_k) & R^{m,n}_{22}(\xi_1+a_e,\xi_2,t_k)\end{bmatrix} \quad \cdots\cdots(38)$$

For the concise expression, we define that

$$\bar{\boldsymbol{V}}^{M,N}_{m,k}=\begin{bmatrix}\bar{V}^{M,N}_{11}(\xi,t_k|e,m) & \bar{V}^{M,N}_{12}(\xi,t_k|e,m)\\ \bar{V}^{M,N}_{21}(\xi,t_k|e,m) & \bar{V}^{M,N}_{22}(\xi,t_k|e,m)\end{bmatrix} \quad \cdots\cdots(39)$$

The coordinates transformation of this from the local to the general coordinates results in

$$\boldsymbol{V}^{M,N}_{\alpha,\beta}=\begin{bmatrix}V^{M,N}_{11} & V^{M,N}_{12}\\ V^{M,N}_{21} & V^{M,N}_{22}\end{bmatrix}=\begin{bmatrix}\cos\theta & \sin\theta\\ -\sin\theta & \cos\theta\end{bmatrix}^T\begin{bmatrix}\bar{V}^{M,N}_{11}\bar{V}^{M,N}_{12}\\ \bar{V}^{M,N}_{21}\bar{V}^{M,N}_{22}\end{bmatrix}\begin{bmatrix}\cos\theta & \sin\theta\\ -\sin\theta & \cos\theta\end{bmatrix} \quad \cdots(40)$$

in which θ is the angle of the rotation of the local coordinates from the general coordinates system.

6. SUBSTRUCTURE FORMULATION FOR COUPLED DOMAINS

Suppose an incidence of the in-plane wave, whose displacement is provided with $\boldsymbol{u}^I$, to a site of irregular configuration. The topography like a canyon generates the diffracted waves. The stress freecondition at the surface of the field also gives a wave reflection. The superimposition of these waves on the incident wave yields the total wave field, leading to the governing equation as

$$\varepsilon_{\alpha\beta}(\boldsymbol{x})\boldsymbol{u}_\alpha(\boldsymbol{x},t)=\int_b\boldsymbol{U}_\alpha((\boldsymbol{y},t;\boldsymbol{x})*\boldsymbol{t}_\alpha(\boldsymbol{y},t)db(\boldsymbol{y})-p.v.\int_b\boldsymbol{T}_{\alpha\beta}(\boldsymbol{y},t;x)*\boldsymbol{u}_\alpha(\boldsymbol{y},t)db(\boldsymbol{y})+\boldsymbol{u}^I_\alpha(\boldsymbol{x},t) \quad \cdots\cdots(41)$$

The discretized form is then expressed by

$$\boldsymbol{H}^0\boldsymbol{U}^K-\boldsymbol{G}^0\boldsymbol{T}^K=-\boldsymbol{F}^K+\boldsymbol{U}^{IK} \quad \cdots\cdots(42)$$

or introducing this the incident wave field results in

$$\boldsymbol{H}^0(\boldsymbol{U}^K-\boldsymbol{U}^{IK})-\boldsymbol{G}^0(\boldsymbol{T}^K-\boldsymbol{T}^{IK})=-\boldsymbol{F}^K \quad \cdots(43)$$

in which $\boldsymbol{U}^K$ and $\boldsymbol{T}^K$ are the displacements and tractions associated with nodes on the irregular boundary as well as those placed on the free surface, and $\boldsymbol{H}^0$ and $\boldsymbol{G}^0$ are determined accordingly ; $\boldsymbol{U}^{IK}$ and $\boldsymbol{T}^{IK}$ denote respectively the discretized displacement and traction values at the above nodes for a specified incident wave field.

For the wave field analysis of two different domains coupled like an alluvium on a uniform halfspace, the substructure procedure is used. Referring to the illustration in **Fig.3**, the separated alluvium portion (Domain $\bar{D}$) is characterized by

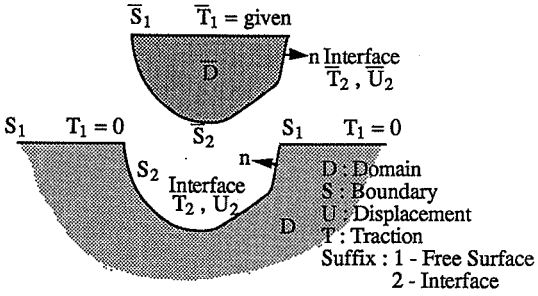

Fig.3 Substructuring for coupled domains.

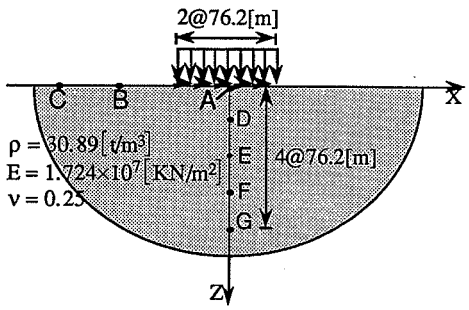

Fig.4 Halfspace under a sudden uniform strip surface load.

the boundary equation Eq.(31). After differentiating nodes at the free surface (indicated by subscript 1) from those on the interface (by subscript 2), we get

$$\begin{bmatrix} \bar{H}^0_{11} & \bar{H}^0_{12} \\ \bar{H}^0_{21} & \bar{H}^0_{22} \end{bmatrix} \begin{Bmatrix} \bar{U}^K_1 \\ \bar{U}^K_2 \end{Bmatrix} - \begin{bmatrix} \bar{G}^0_{11} & \bar{G}^0_{12} \\ \bar{G}^0_{21} & \bar{G}^0_{22} \end{bmatrix} \begin{Bmatrix} \bar{T}^K_1 \\ \bar{T}^K_2 \end{Bmatrix} = - \begin{Bmatrix} \bar{F}^K_1 \\ \bar{F}^K_2 \end{Bmatrix} \quad \cdots\cdots (44)$$

The exterior halfspace (Domain D) should be treated only for the scattering wave, not including incident wave, so that it is governed by

$$\begin{bmatrix} H^0_{11} & H^0_{12} \\ H^0_{21} & H^0_{22} \end{bmatrix} \begin{Bmatrix} U^K_1 - U^{IK}_1 \\ U^K_2 - U^{IK}_2 \end{Bmatrix} - \begin{bmatrix} G^0_{11} & G^0_{12} \\ G^0_{21} & G^0_{22} \end{bmatrix} \begin{Bmatrix} T^K_1 - T^{IK}_1 \\ T^K_2 - T^{IK}_2 \end{Bmatrix} = - \begin{Bmatrix} F^K_1 \\ F^K_2 \end{Bmatrix} \quad \cdots\cdots (45)$$

Condensing out other variables than those related to their interface, the governing equations for the individual domains are expressed by the interface variables as unknown quantities.

$$\bar{A}U^K_2 + \bar{B}T^K_2 = \bar{P}^K, \; AU^K_2 + BT^K_2 = P^K \quad \cdots\cdots (46), (47)$$

in which A, B, P ; $\bar{A}, \bar{B}, \bar{P}$ are properly determined. The continuity condition must be satisfied to make an original coupled domain such that

$$U^K_2 = \bar{U}^K_2, \; T^K_2 + \bar{T}^K_2 = 0 \quad \cdots\cdots (49), (50)$$

The solution is therefore obtained first for the interface nodes and then for the surface nodes along the free surface through the recovery process by use of Eqs.(44) and (45).

7. NUMERICAL EXAMPLES

Two example studies are demonstrated as the application of the present formulation to the boundary-initial value problems ; one is a Lamb's problem for a sudden surface strip loading and the other is a seismic wave propagation problem at irregular sites. The BEM computation is based on the 0-th order straight line elements. The discretization rule claims that the elements length should be less than 1/6 of the concerned wave length. The constant time variation is taken for the stepping algorithm for both example studies. Then, the coefficients A and B in Eqs.(19) and (20) are given as follows :

$$A_0 = \frac{t-z}{2}, \; A_1 = -t, \; A_2 = z, \; A_3 = x, \; A_4 = 0$$

$$B_0 = \frac{1}{2}, \; B_1 = 0, \; B_2 = -1, \; B_3 = 0, \; A_4 = 0$$

Example 1 : Halfspace under sudden uniform strip surface loads

First, an attention is addressed to giving information about the accuracy of the present BEM solution when applied to halfspace elastodynamic problems. Consider a sudden loading of a vertical/horizontal uniform strip traction to act as a Heaviside step function $H(t)$ with intensity of 6.89 $\times 10^4$ KN/m^2 over a width $2a = 76.2$ m on the surface, as illustrated in **Fig.4**. The medium has properties of the Young's modulus $E = 1.724 \times 10^7$ KN/m^2, the mass density $\rho = 30.89$ t/m^3, and the Poisson's ratio $\nu = 0.25$. We are interested in the interior response as well as the surface response.

Fig.5.a and b give those at surface locations indicated in **Fig.4**. The numerical results are compared with those obtained by Mansur (1983) (only for U_{zz} component), and Takemiya and Guan (1993). The former BEM which utilizes the Stokes'solution paid due attention to the causality of the wave propagation, although the numerical procedure was taken for the involed space integration. In the latter integral transform method, besides the causality, the singularity of the Rayleigh wave front is treated analytically through the contour integration procedure. The details are referred to in the respective work. Therefore the discrepancies between the present BEM solution and the integral transform method may be interpreted due to the discretization on the free surface since the BEM solutions shown are based on the fullspace Green's function. It is noted that the BEM solution when sufficient numbers of free

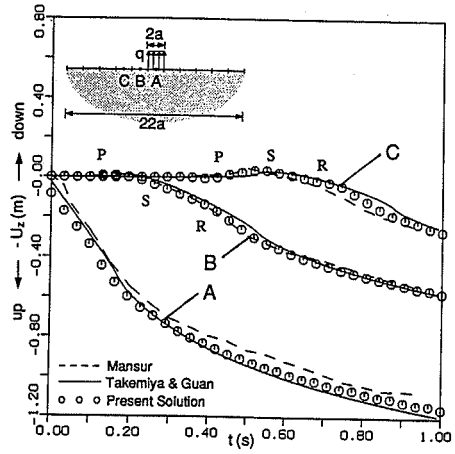

(a) Uz : Vertical displacement due to vertical load

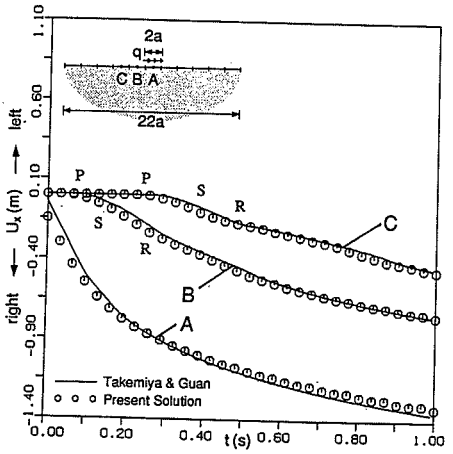

(b) Ux : Horizontal displacement due to horizontal load

Fig.5 Surface displacement responses.

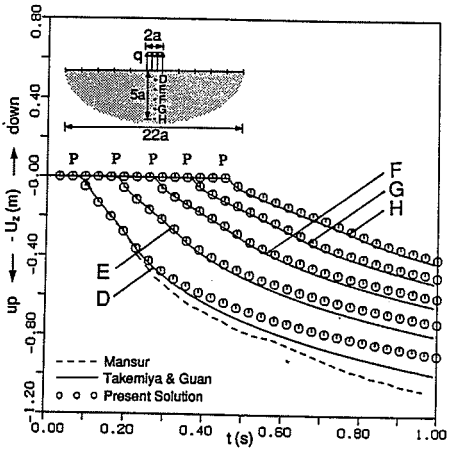

(a) Uz : Vertical displacement due to vertical load

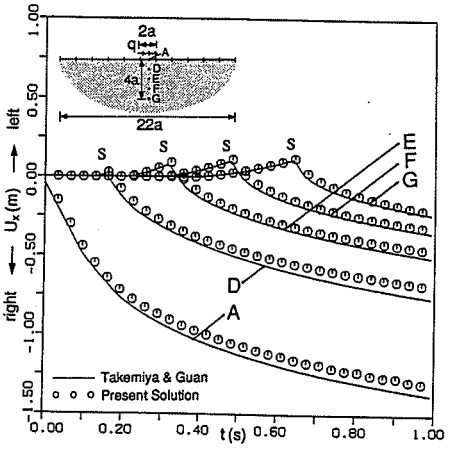

(b) Ux : Horizontal displacement due to horizontal load

Fig.6 Interrior displacement responses.

surface nodes are placed over substantial side ranges, as depicted in the inlet figure, compares well with the solution from the integral transform method. In the figures we notice cleary the arrival time for the P-wave (as marked by the letter P) but not for the S-wave and the Rayleigh wave. However, we can give these waves arrival time as marked by the letter S and R according to the velocity ratios $V_P/V_S=1.732$, $V_R/V_S=0.919$ for the model under consideration. The Rayleigh wave propagation is very obscure for distributed loads in the vicinity of loaded area, for instance at location C at which $x/a=4$, in contrast to line loads.

Fig.6.a and b correspond to the responses at locations below the the center of the loaded area. The arrival times of the P and SV waves are clearly noted, satisfying the causality correctly but obscure for the Rayleigh wave. In **Fig.6**.a for the vertical displacement U_{zz} due to vertical load, no diplacement can be observed until the P wave reaches the observation point. The increasing displacement after the P wave arrival indicates that the focus displacement is dominated by the that wave. The ever increasing nature of response with time does happen only for the 2-dimensional problem but not for the 3-dimensional problem in which the asymptote exists. In **Fig.6**.b the horizontal displacement U_{zz} due to the horizontal loading at the same locations shows that a small opposite displacement appears first when the P wave arrives at the focus location and reaches the peak value when the SV wave arrives and then follows the same directional response with the loading and increases gradually with time. This substantiates the fact that the focus points are domated by the shear wave.

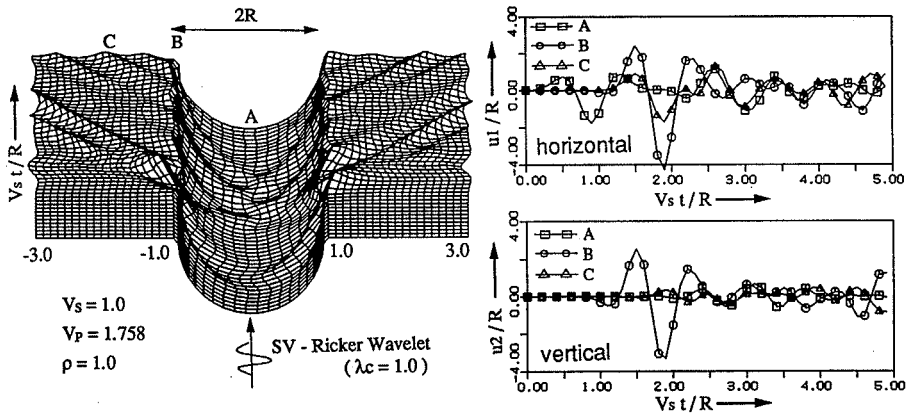

(a) General responce feature (b) Time history

Fig.7 Wave scattering and propagation due to a canyon.

Example 2 : Seismic wave scattering and propagation at irregular site topography

The second numerical computation was conducted to show the wave scattering and propagation at various site irregularities ; a canyon and an alluvium deposit of semi-circular cross section. A Ricker wavelet is employed as an incident wave to such irregular sites to investigate the wave scattering and propagation at transient state. A vertical *SV* wave incidence is assumed. The normalized wave length $\lambda_c=1$ is assumed which means that the incident wave length equals the surface width of the irregular site. Other dimensionless input data used are indicated in the concerned figures.

Canyon : In Figs.7.a and b the scattering waves due to the wave reflection and refraction at the semi-circular canyon surface are clearly shown. The general response features are depicted in **Fig.7**.a at each progressive time step in the 2-dimensional way, and the time histories at focused surface locations, as marked by letters *A*, *B* and *C*, are shown in **Fig.7**.b to give an easy comparison among them. We note that the first wave arrival time is determined by the distance from the incident wave front to the free surface. Then the wave scattering takes place. The smooth semi-circular stress free boundary reflects incident wave back into the soil medium within a certain range of direction, besides those downward from the horizontal free side surface. As the result of these superimpositions, the late wave arrivals appear, like originating from the edges of the canyon, and they propagate both outward along the horizontal surface and inward along the canyon surface as well. The outward-going waves remain along a longer distance while the inward-going waves diminish and die off after they meet at the canyon bottom from both sides. The biggest peak appears at the edge, followed by the nearby surface outside the canyon, and the smallest peak at the bottom inside of it. The similar responce characteristis are observed for the *SH* wave incidence[15].

Alluvium : Figs.8.a and b give the scattering/propagation wave field for a semi-cirular alluvium. We observe that the response features are quite different from those at the canyon above mentioned. Due to the successive wave reflections both at the free surface and at the bottom of the alluvium, the more complicated wave superimposition takes place within it, generating local surface waves and resulting in a longer total wave duration. **Fig.8**.b indicates that significantly amplified peak response is attained at the alluvium surface center. As is clearly observed from **Fig.8**.a most of the waves are trapped inside the alluvium and the outward going waves are less noticeable in contrast to the significance for the canyon case. This will be better interpreted in the harmonic response analysis as indicated in the work by Takemiya, Tomono, Ono and Suda[16] (1992).

8. CONCLUSION

In the present paper, the authors extended the previous work on scalar wave problems[12] to elastodynamic problems, developing the closed-form 2-dimensional fullspace Green functtion for specifically distributed forces, as expressed by the multinormal functions. The scalar wave potentials for the *P* and *SV* (a component associated with the plane wave) waves are introduced for expressing the concerned fundamental solution. The procedure is to utilize the Fourier-Laplace domain transform and then the inversion from the

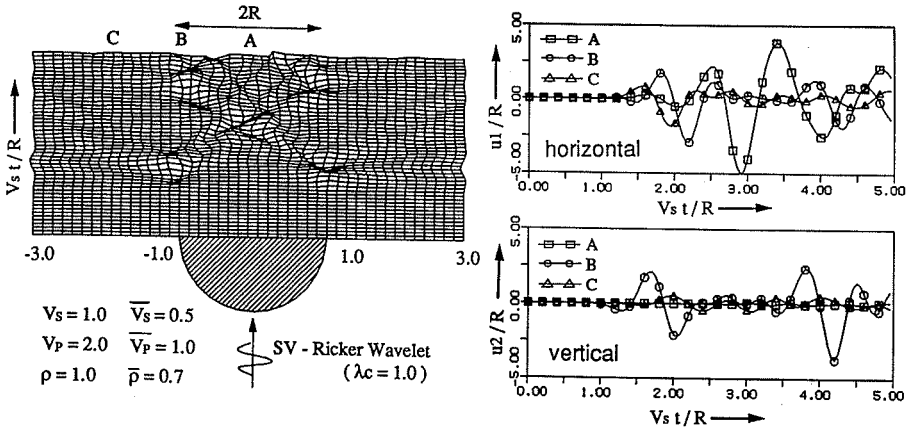

(a) General responce feature (b) Time history

Fig.8 Wave scattering and propagation due to an alluvium.

Cagniard-de Hoop method. The singularity involved in the time-space domain solutions due to the body wave front are eliminated analytically and the causality is fully taken into account. The present analytical solution can be directly used to the time domain boundary element method as the kernal function for the 2-dimensional halfspace elastodynamic problems, and guarantees the accuracy and requires less computation time when compared with the conventional procedure. Numerical computation is performed for the transient response of the Lamb's problem due to surface strip loading of Heaviside time variation. Also conducted is the wave scattering and propagation for a Ricker wavelet incidence at canyon and alluvium of semi-circular cross-section. The similar responce characteristics are observed as for the *SH* wave incidence[15].

Appendix A : Displacements and Stresses

For the displacement computation from Eq.(16), we need to evaluate Eq.(17) and its derivative. In general, we define

$$\frac{\partial^i\partial^i}{\partial x^i\partial t_\alpha^i}\boldsymbol{R}^{m,n}=E(m,i)E(n,j)\left\{1,\frac{\partial}{\partial_z}\right\}X^{m-i}(x)*V(x,z,t_\alpha)*T^{n-j}(t_\alpha)$$
$$=E(m,i)E(n,j)\boldsymbol{R}^{m-i,n-j}\cdots\cdots(A.1)$$

$$\frac{\partial^2}{\partial z^2}\boldsymbol{P}^{m,n}=-E(m,2)\boldsymbol{P}^{m-2,n}+E(n,2)\boldsymbol{P}^{m,n-2}\cdots\cdots(A.2)$$

and the convolution integral

$$t_\alpha*\boldsymbol{R}^{m,n}=\frac{1}{E(n+k+1,k+1)}\boldsymbol{R}^{m,n+k+1}\cdots(A.3)$$

in which

$$E(n,k)=\begin{cases}\dfrac{n!}{(n-k)!} & if\ n\geq k\\ n! & if\ 0\leq n\leq k\\ 1 & if\ n\leq 1\end{cases}$$

By introducing the following notations,

$$P_\alpha^{m-i,n+j}\equiv\frac{E(m,i)}{E(n+j,j)}\frac{1}{c_\alpha^{n+2}}P^{m-i,n+j}(x,z,t_\alpha)\cdots\cdots(A.4)$$

$$Q_\alpha^{m-i,n+j}\equiv\frac{E(m,i)}{E(n+j,j)}\frac{1}{c_\alpha^{n+2}}Q^{m-i,n+j}(x,z,t_\alpha)\cdots\cdots(A.5)$$

we obtain the explicit expressions for displacements and stress components at field point as follows :

$$\rho u_{xx}^{m,n}=[P_1^{n-2,n+2}-P_1^{m-2,n+2}]+P_2^{m,n}\cdots(A.6.a)$$

$$\rho u_{xz}^{m,n}=\rho u_{xz}^{m,n}\cdots\cdots(A.6.b)$$

$$\rho u_{zz}^{m,n}=-[P_1^{m-2,n+2}-P_2^{m-2,n+2}]+P_1^{m,n}\cdot(A.6.c)$$

$$\sigma_{xxx}^{m,n}=\rho(c_1^2-2c_2^2)(u_{xx,x}^{m,n}+u_{xz,z}^{m,n})+2\rho c_2^2u_{xx,x}^{m,n}$$
$$=2c_2^2[P_1^{m-3,n+2}-P_2^{m-3,n+2}]+(c_1^2-2c_2^2)P_1^{m-1,n}+2c_2^2P_2^{m-1,n}\cdots\cdots(A.7.a)$$

$$\sigma_{zzz}^{m,n}=\rho c_2^2(u_{xx,z}^{m,n}+u_{zz,z}^{m,n})=c_2^2\{[2Q_1^{m-2,n+2}-Q_2^{m-2,n+2}]+Q_2^{m,n}\}\cdots\cdots(A.7.b)$$

$$\sigma_{zxz}^{m,n}=\rho c_2^2(u_{xx,x}^{m,n}+u_{zz,z}^{m,n})$$
$$=-c_2^2\{-[2P^{m-3,n+2}-P_2^{m-3,n+2}]+[2P_1^{m-1,n+2}-P_2^{m-1,n+2}]\}\cdots\cdots(A.7.c)$$

$$\sigma_{zxx}^{m,n}=\sigma_{zxx}^{m,n}\cdots\cdots(A.7.d)$$

$$\sigma_{xzz}^{m,n}=\sigma_{zxz}^{m,n}\cdots\cdots(A.7.e)$$

$$\sigma_{zzz}^{m,n}=\rho(c_1^2-2c_2^2)(u_{xx,x}^{m,n}+u_{zz,z}^{m,n})+2\rho c_2^2u_{zz,z}^{m,n}$$
$$=2c_2^2[P_1^{m-3,n+2}-P_2^{m-3,n+2}]-2c_2^2P_2^{m-1,n}$$

$$+c_1^2 P_1^{m-1,n} \quad \cdots\cdots (A.7.f)$$

$$\sigma_{xxz}^{m,n}=\rho(c_1^2-2c_2^2)(u_{xz,x}^{m,n}+u_{zz,z}^{m,n})+2\rho c_2^2 u_{xz,x}^{m,n}$$
$$2c_2^2[Q_1^{m-3,n+2}-Q_2^{m-3,n+2}]$$
$$+(c_1^2-2c_2^2)Q_1^{m-1,n} \quad \cdots\cdots (A.7.g)$$

$$\sigma_{zzz}^{m,n}=\rho(c_1^2-2c_2^2)(u_{xz,x}^{m,n}+u_{zz,z}^{m,n})+2\rho c_2^2 u_{zz,z}^{m,n}$$
$$=-2c_2^2[Q_1^{m-3,n+2}-Q_2^{m-3,n+2}]$$
$$+c_1^2 Q_1^{m,n} \quad \cdots\cdots (A.7.h)$$

Appendix B : $\bar{V}_{k,j}^{M,N}(\xi,t_k|e,m)$ and $R_{k\pm}^{m,n}$

$$\bar{V}_{1,k}^{0,0}=\frac{1}{2}\{(R_{(k+1),+}^{0,0}-R_{k,+}^{0,0})-(R_{(k+1),-}^{0,0}-R_{k,-}^{0,0}) \quad \cdots\cdots (B.1.a)$$

$$\bar{V}_{1,k}^{0,1}=\frac{1}{2}\{(R_{(k+1),+}^{0,0}-2R_{k,+}^{0,1}+R_{(k-1),+}^{0,1})$$
$$-(R_{(k+1),-}^{0,0}-2R_{k,-}^{0,1}+R_{(k-1),-}^{0,1})\} \cdots (B.1.b)$$

$$\bar{V}_{1,k}^{1,0}=-\frac{1}{4}\{(R_{(k+1),+}^{1,0}-R_{k,+}^{1,0})-(R_{(k+1),-}^{1,0}-R_{k,-}^{1,0})\}$$
$$+\frac{1}{2}\{R_{(k+1),+}^{0,0}-R_{k,+}^{0,0}\} \quad \cdots\cdots (B.1.c)$$

$$\bar{V}_{2,k}^{1,0}=\frac{1}{4}\{(R_{(k+1),+}^{1,0}-R_{k,+}^{1,0})-(R_{k+1),-}^{1,0}-R_{k,-}^{1,0})\}$$
$$-\frac{1}{2}\{R_{(k+1),-}^{0,0}-R_{k,-}^{0,0}\} \quad \cdots\cdots (B.1.d)$$

$$\bar{V}_{1,k}^{1,1}=-\frac{1}{4}\{(R_{k+1),+}^{1,1}-2R_{k,+1}^{1,1}+R_{(k-1),+}^{1,1})$$
$$-(R_{(k-1),-}^{1,1}-2R_{k,-}^{1,1}+R_{(k-1),-}^{1,1})$$
$$-(R_{(k+1),-}^{1,0}-R_{k,-}^{1,0})\}+\frac{1}{2}\{R_{(k+1),-}^{0,1}$$
$$-2R_{k,+}^{0,1}+R_{(k-1),+}^{0,1}\} \quad \cdots\cdots (B.1.e)$$

$$\bar{V}_{2,k}^{1,1}=\frac{1}{4}\{(R_{(k+1),+}^{1,1}-2R_{k,+}^{4,1}+R_{(k-1),+}^{1,1})$$
$$-(R_{(k+1),-}^{1,1}-2R_{k,-}^{1,1}+R_{(k-1),-}^{1,1})-(R_{(k+1),-}^{1,0}$$
$$-R_{k,-}^{1,0})\}-\frac{1}{2}\{R_{(k+1),-}^{0,1}-2R_{k,-}^{0,1}+R_{(k-1),-}^{0,1}\}$$
$$\cdots\cdots (B.1.f)$$

REFERENCES

1) Cruse, T.A. and F.J. Rizzo : A direct formulation and numerical solution of the transient elastodynamic problems I, J. Math. Anal. Appl. 22, 244-259, 1968.
2) Lamb, H. : On the propagation of tremors on the surface of an elastic solid, Philos. Trans. Royal Soc, London Ser. A 203, 1-42, 1904.
3) Manolis, G.D. and D.E. Beskos, : Dynamic stress concentration studies by boundary integrals and Laplace transform, Int. J. Num. Mech. Eng. 17, 573-599, 1981.
4) Niwa, Y., S. Kobayashi, and T. Fukui : Application of integral equation method to some geomechanical problems, Proc. 2nd Int. Conf. Num. Meth. Geomech., 120-131, ASCE, 1976.
5) Cole, D.M., D.D. Kosloff and J.B. Minster : A numerical boundary integral equation method for elastodynamics. I, Bull. Seism. Soc. Am., 68.5, 1331-1357, 1978.
6) Niwa, Y., T. Fukui, S. Kato and K. Fujiki:An application of the integral equation method to two-dimensional elastodynamics, Theor. Appl. Mecha., 28, Univ. of Tokyo Press, 281-290, 1980.
7) Manolis, G. : A comparative study on three boundary element method approaches to problems in elastodynamics, Int. J. Num. Meth. Eng.,19, 73-91, 1983.
8) Karabalis, D.L. and D.E. Beskos : Dynamic response of 3-D rigid surface foundations by time domain boundary element method, Earthq. Eng. Struc. Dyn., 12, 73-93, 1984.
9) Mansur, W.J. and C.A. Brebbia : Further Developments on the Solution of the Transient Scalar Wave Equation, Topics in Boundary Element Research, Ed. by Brebbia, C.A., Chap.4, 87-123, 1985.
10) Israil, A.S.M. and P.K. Banerjee : Advanced development of time-domain BEM for two-dimensional scalar wave propagation, Int. J. Numer. Methd. Eng.,29, 1003-1020, 1989.
11) Mansur, W.J. : A time Stepping technique to solve wave propagation problems using the boundary element method, Ph. D Thesis, University Southampton, Southampton, 1983.
12) Wang, C.Y. and H. Takemiya : Analytical elements of time domain BEM for two-dimensional scalar wave problems, Int. J. Numr. Methd. Eng.33, 1737-1754, 1992.
13) de Hoop, A.T. : The surface line source problem, Appl. Sci. Res. B8, 349-356, (1959/1960).
14) Takemiya, H. and. F. Guan : Transient Lamb's solution for surface strip impulses, to appear J. Eng. Mech. Div., ASCE, 1993.
15) Takemiya, H., C.Y. Wang and A. Fujiwara : Two-dimensional transient and steady state response of topographically irregular site due to SH Wave, Proc. JSCE, No.450 / I-20, 171～180, 1992.7. (in Japanese)
16) Takemiya, H., T. Tomono, M. Ono and K. Suda : 2-D Irregular site response characteristics by BEM-FEM hybrid analysis, Proc. JSCE, No.450 / I-20, 63～74, 1992.7.

(Received August 7. 1992)

Structural Eng./Earthquake Eng. Vol. 10, No. 1, 23s—33s, April 1993
Japan Society of Civil Engineers (Proc. of JSCE No. 465/I—23)

分布載荷による2次元弾性体の基本解と半無限平面問題のBEM遷移応答解析

竹宮宏和・王　燦雲・藤原章広

本論文は，一様な弾性体へ帯状分布載荷を衝撃的に与えたときの変位・応力の基本解を評価したものである．載荷力は超関数で表現している．解法はFourier-Laplace変換法をとり，逆変換のためにCagniard-de Hoop法を用いている．応用例としてLambの問題と不整形地盤の地震波の散乱問題を扱っている．